
Numerical test of few-qubit clock protocols

Till Rosenband

Ion Storage Group,
National Institute of Standards and Technology,
325 Broadway, Boulder, CO 80305
E-mail: trosen@boulder.nist.gov
Contribution ICOLS 2011

Abstract The stability of several clock protocols based on 2 to 20 entangled atoms is evaluated numerically by a simulation that includes the effect of decoherence due to classical oscillator noise. In this context the squeezed states proposed by André, Sørensen and Lukin [PRL 92, 239801 (2004)] offer reduced instability compared to clocks based on Ramsey's protocol with unentangled atoms. When more than 15 atoms are simulated, the protocol of Bužek, Derka and Massar [PRL 82, 2207 (1999)] has lower instability. A large-scale numerical search for optimal clock protocols with two to eight qubits yields improved clock stability compared to Ramsey spectroscopy, and for two qubits performance exceeds the analytically derived protocols. In the simulations, a laser local oscillator decoheres due to flicker-frequency ($1/f$) noise. The oscillator frequency is repeatedly corrected, based on projective measurements of the qubits, which are assumed not to decohere with one another.

Keywords: Quantum metrology, spin-squeezing, atomic clocks

1 Introduction

Atomic clocks are intrinsically quantum measurement devices, and it is an open question to what degree quantum many-body states can improve clock operation. Squeezed states were first discussed in the context of optical interferometers with improved resolution [1]. Subsequently, spin-squeezed input states [2] were considered for improved frequency resolution in atomic clocks [3, 4]. Further studies simultaneously optimized the initial quantum state with the clock's measurement basis [5] to achieve frequency resolution that scales as the Heisenberg limit.

In atomic clocks, the highest accuracies are currently reached with pairs of trapped ions [6] where the atom-number is difficult to increase without loss of accuracy. Experiments of similar construction have demonstrated arbitrary unitary transformations of ion-qubit pairs [7]. Therefore, „quantum gain”, where improved performance is extracted from a small number of entangled atoms in clocks, may have practical significance.

This study focuses on the projection-noise-limited frequency stability of passive atomic clocks¹, where the classical oscillator is the only source of decoherence, and the atomic qubits are assumed not to decohere with one another. This situation has been addressed for the case of squeezed states with large qubit numbers [9], and for general quantum states and measurement bases, also in the limit of large qubit numbers [5]. Experimental trapped-atom optical clocks that are based on resonances of metastable excitations share this decoherence mechanism when inter-atom decoherence from interactions, spontaneous emission, and background-field fluctuations can be neglected. In optical atomic clocks the oscillator frequency is derived from laser-stabilization cavities that have an intrinsic thermal noise floor [10] whose power-spectrum of frequency-fluctuations scales as $1/f$. This fundamental thermal-noise floor serves as the model for oscillator decoherence. Note that models of decoherence and oscillator noise are essential ingredients for studies of optical-clock stability, where the uncertainty of the atom-oscillator phase difference is typically of order one radian. In contrast, the atom-oscillator phase difference in many microwave atomic clocks is of order one milliradian, and oscillator noise plays a different role.

2 Clock model

The simulated clocks are generalizations of Ramsey's clock protocol [11]. Each clock contains N qubits whose states are the ground state $|0\rangle = \begin{pmatrix} 1 \\ 0 \end{pmatrix}$ and the excited state $|1\rangle = \begin{pmatrix} 0 \\ 1 \end{pmatrix}$. Ramsey's protocol, as considered here, consists of repeated application of the following steps²:

1. Prepare initial state. All qubits are placed in the state $\psi_1 = \begin{pmatrix} 1 \\ -1 \end{pmatrix} \sqrt{2}$ which is the state $\begin{pmatrix} 1 \\ 0 \end{pmatrix}$ after rotation by $\pi/2$ about the Bloch-sphere x-axis.
2. Free evolution for a period T where a phase difference of ϕ accumulates between the oscillator and the qubits $\psi_2 = \begin{pmatrix} 1 & 0 \\ 0 & e^{-i\phi} \end{pmatrix} \psi_1$.
3. Measure final state by rotating the qubits by $\pi/2$ about the Bloch-sphere y-axis, and counting the number of excited-state qubits. This corresponds to measuring ψ_2 in the basis $a_1 = \begin{pmatrix} 1 \\ -1 \end{pmatrix} \sqrt{2}$, $a_2 = \begin{pmatrix} 1 \\ 1 \end{pmatrix} \sqrt{2}$.
4. Adjust the oscillator frequency by an amount that depends on the measurement outcome in step 3.
5. Add a random variable to the oscillator frequency to model its $1/f$ noise floor³.

In this description the Bloch-sphere rotation directions are defined by the oscillator phase. Thus, when the oscillator accumulates a phase error during the free evolution period, this is modeled as the phase ϕ that is applied differentially to the two states of each qubit in step 2.

¹ In passive atomic clocks a classical oscillator is frequency-stabilized to an atomic resonance. In active atomic clocks such as masers, the clock signal is produced directly by the atoms. Active optical clocks may have a different type of noise floor [8].

² $\pi/2$ rotations are assumed to be infinitesimally short.

³ In this study, the oscillator frequency has a probe cycle to probe cycle variance of 2 Hz^2 , independent of T , corresponding to a flat Allan deviation of 1 Hz. This noise level is chosen for convenience, and is of similar magnitude to the experimental oscillator noise in optical clocks.

The above sequence can be understood as a measurement of the atom-oscillator frequency difference in steps 1 to 3, followed by a correction of the oscillator frequency. Atomic projection noise in step 3 limits the measurement stability to [12]

$$\sigma_f(\tau) = \frac{1}{2\pi\sqrt{NT\tau}}, \quad (1)$$

where $\sigma_f(\tau)$ is the standard deviation of the clock frequency after it has been averaged over the period τ , with respect to the true frequency of the atoms. In order to minimize σ_f , one should maximize the free evolution period T . However, when T is too large, it is possible for frequency errors of $\pm 2\pi/T$ to accumulate undetected, because the atomic signal is periodic. Such occurrences, called „fringe hops”, limit the duration of T . Note that clock protocols with variable T may avoid fringe hops and allow for improved stability.

Ramsey’s protocol can be generalized in two ways. The first is the use of arbitrary multiqubit states for ψ_1 . When these states reduce the phase measurement uncertainty in the limit of small T , the states are considered spin-squeezed [2, 3]. André *et al.* [9] suggest the states $|\psi_1\rangle = \mathcal{N}(\kappa) \sum_{m=-N/2}^{N/2} (-1)^m e^{-(m/\kappa)^2} |N, m + N/2\rangle$, where κ parameterizes the degree of spin-squeezing, $\mathcal{N}(\kappa)$ provides normalization, and the states $|N, m\rangle$ are the fullysymmetrized states of N qubits containing m excitations.⁴ These initial states improve the stability of simulated clocks (see Section 4). The second generalization consists of the use of other measurement bases. Only initial states and measurement bases in the symmetric subspace spanned by the states $|N, m\rangle$ are considered [5]. Such protocols consist of repeated application of these steps:

1. Prepare initial state ψ_1 .
2. Free evolution for a time-period T . $|N, m\rangle \rightarrow e^{-im\phi} |N, m\rangle$
3. Measure final state by projecting into a measurement basis $\{|a_j\rangle\}$.
4. Adjust the oscillator frequency by an amount that depends on which $|a_j\rangle$ was measured in step 3.

Oscillator noise is simulated as before. This protocol could be further generalized to include the possibility of partial measurements, ancilla qubits, and frequency corrections that depend also on the measurement outcomes from prior cycles. However, such extensions are not considered here. Furthermore, the free-evolution period T is fixed for each protocol instance.

Bužek *et al.* have optimized analytically the initial state ψ_1 and basis $\{|a_j\rangle\}$ for phase measurements in the limit of large N . The authors find⁵

$$|\psi_1\rangle = \sum_{m=0}^N \sqrt{\frac{2}{N+1}} \sin \frac{\pi(m+1/2)}{N+1} |N, m\rangle \quad (2)$$

and

$$|a_j\rangle = \frac{1}{\sqrt{N+1}} \sum_{m=0}^N e^{im\phi(j)} |N, m\rangle, \quad (3)$$

where $\phi(j) = 2\pi j/(N+1)$. Simulated clocks based on this protocol achieve Heisenberg-limited scaling (see Section 4). The phase-shifted basis states where $\phi(j) = 2\pi(j+1/2)/(N+1)$ are also considered, because they offer reduced clock instability when N is odd.

⁴ For example, $|4, 3\rangle = (|0111\rangle + |1011\rangle + |1101\rangle + |1110\rangle)/2$.

⁵ This result holds when phase errors can be considered modulo 2π . When the free-evolution period T is optimized in optical clocks, phase errors beyond 2π must also be taken into account.

The above optimization is for a uniform distribution of oscillator phase errors on the interval $[-\pi, \pi)$, while in experimental clocks the phase error has a distribution that is peaked at $\phi=0$ and drops near zero as ϕ approaches $\pm\pi$. In this work the frequency corrections associated with each basis state are numerically optimized, to account for the non-uniform distribution at the correction stage. Other studies explicitly optimize phase estimation protocols as a function of the prior distribution of phases [13, 16], and this approach is likely to result in more stable few-qubit clock protocols.

3 Numerical search

The generalized protocol described above can be parameterized by an array of real numbers. For each protocol, the expected instability can then be calculated in a Monte Carlo simulation. In the present study, a numerical optimizer adjusts the protocol parameters to find the best performance. This is a difficult numerical problem, because the dimensionality grows quickly with qubit number N , and numerical optimizers are not well suited to optimize the results of Monte Carlo simulations, which contain noise from the randomization process⁶. Nevertheless, this numerical search yields protocols whose performance exceeds that of Ramsey’s protocol for two to eight qubits.

Minimization of the search-space dimensionality is critical. As noted above, only initial states and measurement bases in the symmetric subspace (spanned by the $|N, m\rangle$ states) are considered. For the numerical search, $2N + 1$ real numbers (reals) parameterize the initial state and $N^2 + N$ reals parameterize the measurement basis. Because both unitary operations and measurement bases can be written as orthonormal matrices, their parameterization is nearly identical. Efficient parameterization of unitary operations is described by Tilma and Sudarshan [15]. For the present calculation, extraneous phase degrees of freedom have been removed from the basis states. In addition, $N + 1$ reals parameterize the frequency corrections, and one real parameterizes the free-evolution period T . In total, $N^2 + 4N + 3$ reals parameterize an N -qubit clock. It is believed that a minimal parameterization requires $N^2 + 4N + 2$ reals.

Clock performance is measured as the long-term instability. That is, if the clock runs for many interrogation cycles, how close is the average oscillator-frequency to that of the atomic qubits? The Monte Carlo simulator propagates the clock through 10^5 cycles, and calculates the variance of 100-cycle frequency-averages. Additional steps are taken to ensure that this variance reflects the long-term clock instability. The oscillator noise is pre-computed to have a $1/f$ power spectrum of frequency noise [10, 16] with an Allan deviation [17] of 1 Hz.

It should be noted that for a fixed free-evolution period T , the frequency of all clocks with finite N diverges as a random walk, because undetectable 2π phase jumps (fringe hops) cannot be avoided entirely. Nevertheless the probability of fringe hops can be made small for large but finite numbers of clock cycles. This regime of a large, but finite number of clock cycles describes both real clocks, which do not run forever, and the Monte Carlo simulations in this work.

The search was performed via Nelder-Mead optimization [16] of randomized protocols that meet a performance threshold. All $N^2 + 4N + 3$ parameters were randomly varied for the general search, so that all possible initial states and measurement bases were within the search space. When initial tests yielded good stability, the protocol was run through the optimizer for further refinement. For known protocols, only the frequency corrections and free-evolution period T were varied, as well as the squeezing parameter κ , where applicable. For all protocols, optimal frequency corrections were estimated by assuming a prior Gaussian distribution of

⁶ Performance estimates based on Markov chains would avoid the problem of randomization noise. But because the $1/f$ noise process is non-stationary, a very large state space may be needed for accurate estimates of long-term stability.

frequency errors, and computing the mean frequency associated with each possible measurement outcome $|a_i\rangle$. To these estimates random offsets were added before testing the protocol. In the case of known protocols, certain symmetries are evident, and these symmetries were also enforced for the frequency corrections.

4 Results

Numerical simulations of the clock protocols considered here are summarized in Figure 1(a). Ramsey’s protocol defines the standard quantum limit (SQL), and it is evident that entangled states of two or more qubits can reduce clock instability. The spin-squeezed states suggested by André *et al.* yield the best performance for 3 to 15 qubits, and improve upon the SQL variance by a factor of $N^{-1/3}$. For more qubits, the protocol of Bužek *et al.* further reduces clock variance, because this protocol scales as N^{-1} . The numerical search was run in many parallel threads to find protocols that surpass these analytical protocols, but for two qubits⁷, the clock-variance is only reduced by 1, within the margin of error for this calculation. Although the analytical protocols are within the search space, their performance is not reached by the general search program for $N > 3$, due to the size of the problem. The optimized free-evolution period T for different protocols is shown in Fig. 1(b).

The behavior of the different types of clocks is illustrated in Fig. 2, where it can be seen that the protocol of Bužek *et al.* gains frequency resolution as $1/N$, because each basis state corresponds to a range of phases that shrinks as $1/N$. The squeezed-state protocols are similar to Ramsey’s protocol, but gain frequency resolution near $\phi = 0$ at the expense of decreased resolution near $\phi = \pm\pi/2$. For $N = 2$ the “Search” protocol is very similar to that of André *et al.*

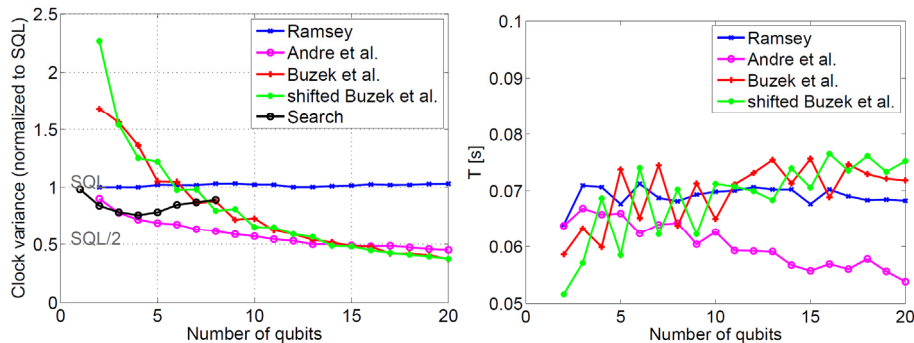


Fig. 1: (color online) **Left:** long-term statistical variance of entangled clocks that contain different numbers of qubits, compared to the standard quantum limit (SQL). The most stable clocks found by the large-scale search are shown as black points. Each point is based on several hours of runtime on NIST’s computing cluster, where typically 2000 processor cores were utilized in parallel. Also shown is the simulated performance of analytically optimized clock protocols. Approximately 15 qubits are required to improve upon the SQL by a factor of two. **Right:** numerically optimized free-evolution period T for clock protocols considered here, when the oscillator noise has an Allan deviation of 1 Hz.

⁷ The probability amplitudes for the different possible states are $Ue^{-i\tau T/\hbar}\psi_1$. Numerically optimized values for two qubits, where Fig. 2 includes the corrections and probe period.

$$U = \begin{pmatrix} -0.486 - 0.039i & 0.708 - 0.132i & 0.335 + 0.363i \\ 0.470 + 0.106i & 0.687 - 0.082i & -0.364 - 0.395i \\ -0.570 + 0.454i & -0.043 + 0.000i & -0.684 + 0.000i \end{pmatrix}, \quad \psi_1 = \begin{pmatrix} -0.572 + 0.000i \\ -0.220 - 0.580i \\ 0.458 - 0.282i \end{pmatrix}$$

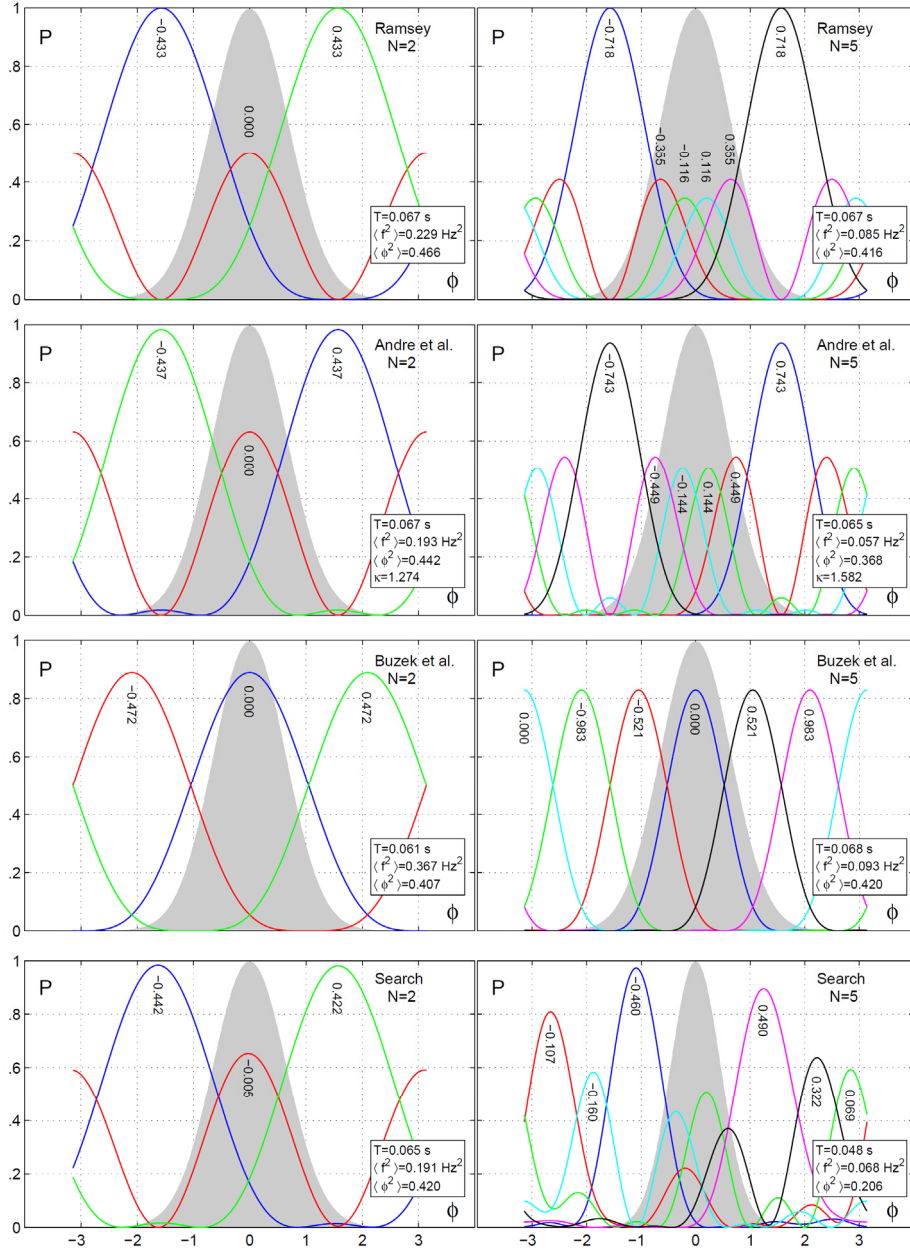


Fig. 2: (color online) Probability (P) of measuring each basis state as a function of the atom-oscillator phase difference (ϕ). Shown are the various protocols for two and five atoms. Each differently colored curve corresponds to a basis state that ψ_1 is projected onto after free evolution. Vertical text near the curves' peaks indicates the optimized phase estimate (ϕ_{Est}). In the simulations, the frequency corrections are $\phi_{\text{Est}}/(2\pi T)$. Shaded in the background is the Gaussian distribution whose variance ($\langle \phi^2 \rangle$) represents the atom-oscillator phase differences that occur in the simulation. Also listed is the optimized probe period T , squeezing parameter κ where applicable, and long-term frequency variance of the clock extrapolated to 1 second. For long-term averages of n seconds, the variance is $\langle \dot{f}^2 \rangle/n$.

5 Conclusion

For accurate ion clocks, further experimental improvements are required to achieve full quantum control of two clock qubits, where the available „quantum gain” appears to be 15 % to 20 %. It is likely that gains of similar magnitude can be derived from easier to implement classical improvements, where the free-evolution period is varied to prevent fringe hops. Such classical protocols will define a new standard quantum limit with which to compare variable probe time, entanglement-based, protocols. It remains an open question how much quantum gain is possible in variable probe-time clocks. Recent theoretical work on efficient quantum-phase estimation [13, 14] may improve upon the protocols considered here [5, 9], especially for three or more qubits.

Acknowledgments

Helpful discussions with S. Lloyd, E. Knill, D. L. Rosenband, and D. J. Wineland are gratefully acknowledged. This work was supported by the DARPA QuASaR program, ONR, and AFOSR. Contribution of NIST, not subject to U.S. copyright.

References

- [1] Special issue on squeezed light in *J. Opt. Soc. Am.* **B 4**, 1450 (1987) 41987.
- [2] M. Kitagawa and M. Ueda, *Phys. Rev. A* **47**, 5138 (Jun 1993).
- [3] D. J. Wineland, J. J. Bollinger, W. M. Itano and D. J. Heinzen, *Phys. Rev. A* **50**, 67 (1994).
- [4] J. J. . Bollinger, W. M. Itano, D. J. Wineland and D. J. Heinzen, *Phys. Rev. A* **54**, R4649 (1996).
- [5] V. Bužek, R. Derka and S. Massar, *Phys. Rev. Lett.* **82**, 2207 (1999).
- [6] C. W. Chou, D. B. Hume, J. C. J. Koelemeij, D. J. Wineland and T. Rosenband, *Phys. Rev. Lett.* **104**, p. 070802 (Feb 2010).
- [7] D. Hanneke, J. P. Home, J. D. Jost, J. M. Amini, D. Leibfried and D. J. Wineland, *Nature Physics* **6**, 13 (2010).
- [8] D. Meiser, J. Ye, D. R. Carlson and M. J. Holland, *Phys. Rev. Lett.* **102**, p. 163601 (2009).
- [9] A. André, A. S. Sørensen and M. D. Lukin, *Phys. Rev. Lett.* **92**, p. 230801 (2004).
- [10] K. Numata, A. Kemery and J. Camp, *Phys. Rev. Lett.* **93**, p. 250602 (2004).
- [11] N. F. Ramsey, *Molecular Beams* (Oxford University Press, 1956).
- [12] W. M. Itano, J. C. Bergquist, J. J. Bollinger, J. M. Gilligan, D. J. Heinzen, F. L. Moore, M. G. Raizen and D. J. Wineland, *Phys. Rev. A* **47**, p. 3554 (1993).
- [13] R. Demkowicz-Dobrzanski, *arXiv:1102.0786* (2011).
- [14] M. Mullan and E. Knill, *arXiv:1107.5347* (2011).
- [15] T. Tilma and E. C. G. Sudarshan, *J. Phys. A* **35**, 10467 (2002).
- [16] J. L. Lennon, *Ecography* **23**, 101 (2000).
- [17] W. J. Riley, *Handbook of Frequency Stability Analysis* (2008). NIST Spec. Pub. 1065.
- [18] M. Galassi *et al.*, *GNU Scientific Library Reference Manual* - 3rd Ed., (2009).